Mass measurements of neutron-rich Rb and Sr isotopes

R. Klawitter,[1,2] A. Bader,[1,3] M. Brodeur,[4] U. Chowdhury,[5] A. Chaudhuri,[1] J. Fallis,[1] A.T. Gallant,[1,6] A. Grossheim,[1] A.A. Kwiatkowski,[7,1] D. Lascar,[1] K. G. Leach,[1] A. Lennarz,[1,8] T.D. Macdonald,[1,6] J. Pearkes,[6] S. Seeraji,[9] M.C. Simon,[10] V.V. Simon,[11] B.E. Schultz,[4] and J. Dilling[1,6]

[1] *TRIUMF, 4004 Wesbrook Mall, Vancouver BC, V6T 2A3 Canada*
[2] *Max Planck Institut für Kernphysik, 69117 Heidelberg, Germany*
[3] *École des Mines de Nantes, 4, rue Alfred Kastler, B.P. 20722, F-44307, Nantes, France*
[4] *Department of Physics, University of Notre Dame, Notre Dame, Indiana 46556 USA*
[5] *Department of Physics, University of Manitoba, R3T 2N2, Winnipeg, Canada*
[6] *Department of Physics & Astronomy, University of British Columbia, Vancouver BC, V6T 1Z1 Canada*
[7] *Cyclotron Institute and Deptartment of Physics and Astronomy, Texas A&M University, College Station, TX 77843, USA*
[8] *Institut für Kernphysik, Westfälische Wilhelms-Universität, 48149 Münster, Germany*
[9] *Department of Chemistry, Simon Fraser University, Burnaby, British Columbia V5A 1S6, Canada*
[10] *Stefan Meyer Institute for Subatomic Physics, Austrian Academy of Sciences, 1090 Vienna, Austria*
[11] *Physikalisches Institut der Universität Heidelberg, 69120 Heidelberg, Germany*

(Dated: September 12, 2018)

We report on the mass measurements of several neutron-rich Rb and Sr isotopes in the $A \approx 100$ region with the TITAN Penning-trap mass spectrometer. Using highly charged ions in the charge state $q = 10+$, the masses of ^{98,99}Rb and $^{98-100}$Sr have been determined with a precision of $6 - 12$ keV, making their uncertainty negligible for r-process nucleosynthesis network calculations. The mass of ^{101}Sr has been determined directly for the first time with a precision eight times higher than the previous indirect measurement and a deviation of 3σ when compared to the Atomic Mass Evaluation. We also confirm the mass of ^{100}Rb from a previous measurement. Furthermore, our data indicates the existance of a low-lying isomer with 80 keV excitation energy in ^{98}Rb. We show that our updated mass values lead to minor changes in the r-process by calculating fractional abundances in the $A \approx 100$ region of the nuclear chart.

I. INTRODUCTION

Understanding the production of the heaviest elements found in nature is one of the most challenging open question for all of physics [1]. Although it is generally understood that half of the elements heavier than iron (Z > 26) are synthesized in a series of rapid nuclear reactions and subsequent decays (r-process) in short, violent stellar explosions, there is no consensus on the exact astrophysical events responsible [2, 3]. The r-process is fueled by an extreme overabundance of neutrons ($n_n > 10^{20}\text{cm}^{-3}$) in a hot ($T \gtrapprox 10^9$ K) environment, creating very neutron-rich isotopes by sequential, rapid neutron captures (n, γ) which are eventually balanced by photodisintegrations (γ, n). Starting from a seed nuclide, usually around iron, it creates a path through the isotopic chart up to uranium, with β-decays connecting the isotopic chains. When the temperature and neutron density drop, the process "freezes out", and the neutron-rich isotopes β-decay to stability.

The path describing the r-process through the nuclear chart strongly depends on the neutron-separation energies (S_n) of nuclei on and around it. Likely scenarios for the r-process [4] take place in environments where neutron captures and photodisintegrations are much faster than β-decays. Therefore, a $(n, \gamma) \rightleftharpoons (\gamma, n)$ equilibrium is reached in each isotopic chain, and the yields Y_i of neighboring isotopes satisfy the nuclear Saha equation [5]:

$$\frac{Y_1}{Y_2} = n_n \frac{G_1}{2G_2} \left(\frac{A+1}{A} \frac{2\pi\hbar^2}{m_u kT} \right)^{3/2} e^{S_n/kT} \qquad (1)$$

for partition functions G_i, Boltzmann constant k, temperature T, atomic mass unit m_u, and mass number A. Most of the abundance in a chain is carried by one or two "waiting-points" [6] that inhibit capture to heavier nuclei until their β-decay enables further, energetically favorable neutron captures in the next isotopic chain.

Waiting points have a large impact on the final abundance patterns, especially when their neutron number is magic ($N = 50, 82, 126$). In those cases, S_n can drop markedly, and the r-process runs through several, rather long β-decays [7]. S_n for the most likely r-process environment with temperatures of $T \sim 10^9 K$ and neutron densities of $n_n > 10^{20}\text{cm}^{-3}$ are expected to be $2-3$ MeV [4]. The path runs therefore through very neutron-rich, unstable nuclei. These nuclides are challenging to produce in the laboratory and to measure with the required accuracy, as an uncertainty of $10 - 100$ keV on the S_n is required to consider it negligible in r-process models. As a consequence, only a few waiting-point masses have been derived directly [5]. Where direct mass measurements are not yet feasible, the S_n has to be extracted from theoretical models (e.g. [8–10]), which can differ substantially in predicted mass values for nuclei far from stability. One such region of waiting points is assumed to be at $A \approx 100$, $N \approx 60$ where rapid shape transitions are

not well reproduced by theoretical mass models [11, 12]. Experimental mass values for neutron-rich isotopes, especially in the vicinity of r-process waiting points, are crucial to further constrain nucleosynthesis models as well as to help increase the predictive power of mass models far from stability.

Ion traps are well established as the tool of choice for mass measurements of short-lived isotopes [13]. TRIUMF's Ion Trap for Atomic and Nuclear science (TITAN) [14, 15] is optimized to make the fast, precision mass measurements, and it is the only facility of its kind employing an electron beam ion trap (EBIT) to charge-change short-lived isotopes for the pupose of Penning-trap mass spectrometry. In this article we report on Penning-trap mass measurements of ^{98,99}Rb and $^{98-100}$Sr with TITAN and show how the updated mass values change the fractional abundances of the r-process in the $A \approx 100$, $N \approx 60$ region of the nuclear chart.

II. EXPERIMENTAL METHOD

TITAN is coupled to the Isotope Separator and Accelerator (ISAC) [16] facility at TRIUMF, where, for the experiment described, 8 μA of 480 MeV protons were directed onto a uranium carbide target [17] to produce radioactive isotopes. These were then ionized using a surface ion source, extracted, and accelerated to 20 keV beam energy. The neutron-rich Rb/Sr isotopes of interest were subsequently separated by a dipole magnet with a resolving power of up to $m/\delta m \approx 3000$ [18]. After selection the beam of interest was directed to and injected into the TITAN Radio Frequency Quadrupole (RFQ, [19, 20]) cooler and buncher. Here, the accumulated beam was cooled by interacting with a helium buffer gas for a few ten to a few hundred milliseconds, extracted in bunches, and directed towards the electron beam ion trap (EBIT, [21]).

Rb/Sr bunches captured in the EBIT were collisionally ionized further by an electron beam with current $I_e = 100$ mA and energy $E_e = 2.5$ keV, resulting in a distribution of charge states (see Fig. 1). The $q = 10+$ charge state was then selected by time of flight (TOF) with a Bradbury-Nielson gate (BNG, [22]).

After being injected into the measurement Penning trap (MPET), the cyclotron frequency ν_c of the ion of interest was measured using the time-of-flight ion-cyclotron-resonance technique (TOF-ICR, [23], see also Fig. 2). The mass m^+ of an ion in a homogeneous magnetic field with strength B can then be inferred from:

$$2\pi\nu_c = \frac{q \cdot e}{m^+} B, \tag{2}$$

with q being the ion charge state and e the elementary charge. The precision is given by:

$$\frac{\Delta m}{m} = F \cdot \frac{m}{qeBT_{RF}\sqrt{N_{ion}}}, \tag{3}$$

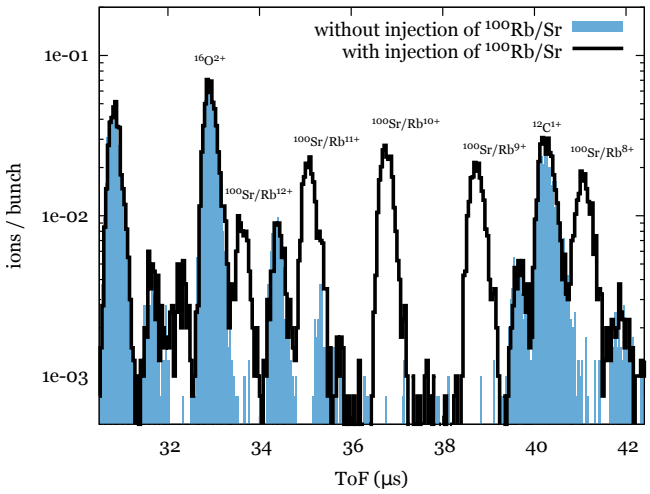

Figure 1. (color online) Typical time-of-flight (TOF) spectrum for ions extracted from the EBIT recorded with a micro-channel plate detector (MCP) just upstream of MPET. Charge state $q = 10+$ (central peak) was used for mass determination of all the isotopes to minimize the amount of ionized residual gas (colored peaks) entering the Penning trap.

where T_{RF} the excitation time, N_{ion} the number of observed ions, and F an apparatus-dependent proportionality constant close to unity for TITAN [24]. The excitation time is restricted by the ion's half-life; the magnetic field is limited technically to $4-10$ T; and, N_{ion} depends on the isotopes' yield and the overall system efficiency. With an EBIT, however, the charge state of radioactive ions can be increased within a few milliseconds, providing a powerful tool for high-precision mass measurements on short-lived isotopes far from stability [25–27]. TITAN is currently the only facility in the world using highly charged ions (HCI) for the purpose of Penning-trap mass spectrometry (PTMS) on short-lived isotopes, bringing unique opportunities and challenges [28]. Since yields for isotopes far from stability are generally low, with rates down to a few ions per second, efficient ion trapping, extraction, and transport become still more important. For the experiment described in this work, total system efficiency was around 0.1%, limiting measurements to isotopes with yields from ISAC of about 10^3 ions/s.

III. ANALYSIS AND RESULTS

To remove the dependency on the magnetic field in eq. 2, the ratio of two cyclotron frequencies:

$$R = \frac{\nu_{c,ref}}{\nu_c} = \frac{q_{ref} \cdot m^+}{q \cdot m^+_{ref}} \tag{4}$$

is recorded, where q, q_{ref} are the charge state and m^+, m^+_{ref} the mass of the ion of interest and of a well-known reference ion respectively. To compute R, we ex-

tracted the cyclotron frequency of the ion of interest and of the reference ion from a fit of a well-known analytic form [23] to the data; see Fig. 2 for an example. The atomic mass m of the isotope can then be calculated from the ratio R using:

$$m = \frac{q}{q_{ref} \cdot R} \cdot (m_{ref} - q_{ref} \cdot m_e + B_{e,ref}) + q \cdot m_e - B_e, \tag{5}$$

where $B_e, B_{e,ref}$ are the atomic binding energy of the ion of interest and reference ion respectively, and m_e is the mass of the electron.

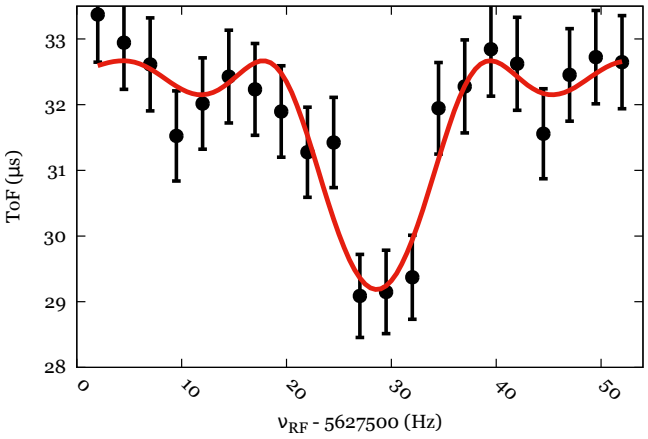

Figure 2. (color online) Time-of-flight (TOF) resonance of ^{101}Sr [$T_{1/2}$ = 118(3) ms]. Black dots: average time-of-flight and associated standard deviation; continous red line: fit [23] to the data.

A number of systematic effects can influence the result and have to be taken into account. Although we selected a specific charge state to minimize background with the BNG, ion bunches from the EBIT contain contaminant ions that will enter the Penning trap (see Fig. 1). Furthermore, HCI can charge exchange with neutral background atoms, creating ions of different charge states inside the trap.

We minimized the effects of contaminants and of more than one trapped ion [29] in a number of ways. Firstly, a 10 ms long dipole cleaning excitation [30] was used to remove known contaminants from the trap. Secondly, the beam transfer rate was adjusted to have, on average, less than one detected ion per measurement cycle. Thirdly, all values are based on an analysis that includes only cycles with one detected ion. The difference in R using all cycles to fit the data as compared to only considering cycles with one detected ion was added as a systematic uncertainty [25]. As the number of total detected ions was low, especially for the shortest-lived isotopes investigated, "count-class"-type analysis [29] could not be used. However, results for species with more than three detected ions per cycle on average were cross-checked using a count-class analysis, showing agreement with the non-count-class analysis to within 0.3σ. Finally, for ion events to be included in the analysis, the ion time of flight had to be within a certain range, 20 μs $\leq t \leq$ 50 μs. This excludes events that are due to light charge-exchange products (e.g. H_2^+) as well as limits the effect of other contaminants. It was found in an off-line study, that contaminants typically populate the TOF spectrum in this range and can be excluded in this way. However, as the correct range cannot be selected unequivocally, the maximal shift in R due to a set of different TOF ranges (20 μs $\leq t \leq$ 40 μs, 20 μs $\leq t \leq$ 60 μs) was added as a systematic uncertainty.

Since the described experiment was performed with HCI, the difference in atomic binding energies of reference ion and ion of interest is on the order of a few hundred eV and has to be taken into account. We used binding energies from [31], with an estimated total uncertainty of 5 eV [12], which can be neglected.

At TITAN, reference ions and ions of interest cannot be measured simultaneously. The reference mass is therefore interpolated linearly from two reference measurements (^{85}Rb in our case), one taken before and one taken after the measurement of the ion of interest. As eq. 5 is valid only for a constant magnetic field, fluctuations over time in the magnetic field will affect the determined mass. For our setup these fluctuations were shown to be below $\Delta R/R$ = 0.2 ppb/h [32]. To reduce their effect the period for a single measurement was limited to 0.5 h. The mass of ^{85}Rb is known to within 5 eV [33] and therefore also negligible.

Systematic uncertainties due to relativistic effects, field inhomogeneities, distortions or misalignment are either proportional to the difference in q/m or m/q of ion of interest and reference ion. To minimize any such effect, we choose a reference m/q as close as possible to the m/q of the species of interest, with $1.038 < \frac{m \cdot q_{\rm ref}}{q \cdot m_{\rm ref}} < 1.070$ by preparing stable ^{85}Rb from the TITAN off-line source [14] in charge state $q = 9+$, where m is given in atomic mass units. Spatial magnetic field inhomogeneities and harmonic distortions as well as misalignment of the magnetic field axis are known to be $\Delta R/R = 3 \cdot 10^{-11}$, and $\Delta R/R = 3 \cdot 10^{-10}$ [32] respectively and can therefore be neglected as well.

Since HCI experience larger velocities inside the Penning trap than SCI, relativistic effects can become important and have to be considered. Following [32] their influence is below $\Delta R/R = 9 \cdot 10^{-10}$ for the results presented and have not been included in the reported uncertainties. To exclude other systematic effects and monitor system performance, we made frequent measurements of the mass of ^{85}Rb^{8+} with ^{85}Rb^{9+} as reference ions, showing good agreement (δm below 0.1σ) with the literature value [33].

The frequency ratios of all measured isotopes relative to ^{85}Rb^{9+} are summarized in Table III, together with the corresponding mass excess and, for comparison, mass excess values found in the literature.

Table I. Frequency ratios of $^{98-100}Rb^{10+}$ and $^{98-101}Sr^{10+}$ isotopes relative to $^{85}Rb^{9+}$ as well as atomic mass excesses. The first uncertainty on the frequency ratio represents the statistical uncertainty multiplied by the reduced-χ^2 of the fit to the data. The second and third uncertainties reflect ambiguities in the choice of time-of-flight range and number of detected ions included in the resonance [25] respectively. The fourth uncertainty in curly brackets represents the quadrature sum of all the uncertainties. For the mass excesses the combined uncertainty is shown. For comparison the last three columns contain mass excess values as determined by ISOLTRAP [34], JYFLTRAP [35], and the values quoted in the AME 2012 [33] .

	$T_{1/2}$ (ms)	# ions	T_{rf} (ms)	Frequency ratio $r = \nu^+_{ref}/\nu$	ME (keV)	ME_{ISOL} (keV)	ME_{JYFL} (keV)	ME_{AME} (keV)
^{98}Rb	114(5)	5737	80	1.038109144(48)(39)(12){63}	-54319.6(5.5)	-54309.4(4.0)		-54318.3(3.4)
^{99}Rb	54(4)	5095	80	1.04874535(07)(08)(03){11}	-51124.6(9.3)	-51120.3(4.5)		-51205(112)
^{100}Rb	51(4)	482	30	1.0594014(09)(11)(06){15}	-46190(140)	-46247(20)		-46547(196)
^{98}Sr	653(4)	6346	80	1.037971485(38)(59)(30){76}	-66416.6(6.7)		-66431(10)	-66426.0(3.7)
^{99}Sr	269(1)	5270	80	1.048615651(46)(54)(21){74}	-62522.4(6.5)		-62524(7)	-62511.9(3.6)
^{100}Sr	202(4)	7110	80	1.05924630(11)(06)(04){13}	-59816(11)		-59828(10)	-59830.1(9.5)
^{101}Sr	118(3)	2760	80	1.06989723(11)(02)(01){11}	-55327.6(9.8)			-55562(81)

A. ^{98}Rb (ground and isomeric state)

We determined the mass excess of the produced state of ^{98}Rb to be −54319.6(5.5)keV, in agreement (0.22σ) with a previous TITAN mass measurement and the Atomic Mass Evaluation (AME 2012) value, but disagreeing (1.85σ) with a recent determination by ISOLTRAP [34].

In an effort to identify a proposed low-lying isomeric state [36], with an estimated excitation energy of ≈ 280(128) keV [33] and $T_{1/2} = 96(3)$ ms, we searched for a characteristic signature [37] within a range of ±2.5 MeV around the known state. However, the observed time-of-flight distribution for ions in resonance is consistent with a predominantly populated very low lying isomeric state of $^{98}Rb^m$ and an admixture of about 30(10)% of the $^{98}Rb^g$ ground state. Using a double-resonance [37] function to fit the data yields an excitation energy of 80 keV and leads to a decrease in the reduced-χ^2 of the fit by about 15%. Due to insufficient resolution the associated uncertainty is about as big as the excitation energy itself.

The discussion about a long-lived isomeric state was recently renewed by results from a collinear laser spectroscopy experiment on ^{98}Rb [38], that used the identical production mechanism. With this in mind we reanalyzed all data from our 2012 publication [12]. The previous experiment used ^{98}Rb in charge state $q = 15$ instead of $q = 10$, giving correspondingly better resolving power. We extracted the mass excesses from a double resonance fit (see figure 3), calculating −54296(20) keV for the isomeric state and −54376(30) keV for the ground state. The relative populations of 35(15)% to 65(15)%, respectively, are in agreement with the values obtained in the collinear laser spectroscopy expermiment [38].

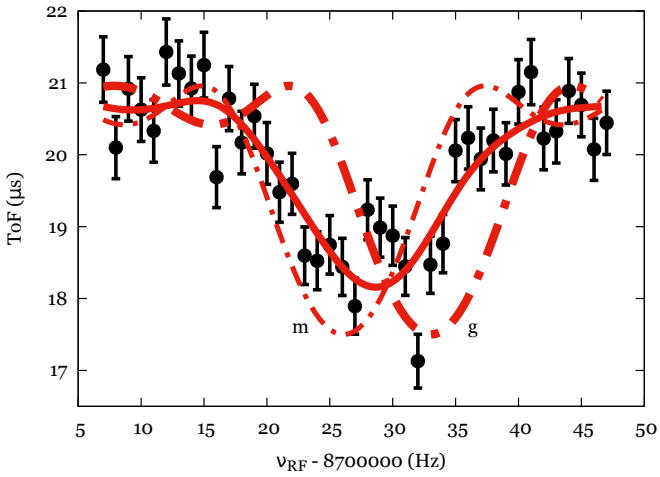

Figure 3. (color online) Black points: All TOF-ICR data for $^{98}Rb^{g,m;q=15+}$ from [12] added. Dashed lines: Individual contributions of $^{98}Rb^{m;q=15+}$ and $^{98}Rb^{g;q=15+}$ respectively as well as fit to both states together (solid line). The reduced-χ^2 for a two-state model is $\chi^2_{r,g+m} = 1.7$ as compared to $\chi^2_r = 2$ for a one-state model.

B. ^{99}Rb

We measured the mass excess of ^{99}Rb [$T_{1/2} = 54(4)$ms] to be −51124.6(9.3) keV, which is in agreement with a recent ISOLTRAP measurement by Manea et al. [34]. Both values agree within 1σ of the value published in the AME 2012 [33, 39] but carry less than a tenth of the uncertainty. The AME 2012 value was adopted from a measurement employing a double-focusing mass spectrometer [40] (with 13% weight) and a determination using the β-endpoint endpoint energy of ^{99}Rb (β^-) ^{99}Sr [41]

(87% weight).

C. ^{100}Rb

We confirm the first PTMS measurement of ^{100}Rb [$T_{1/2}$ = 51(4)] by Manea et al. [34]. Since the amount of ^{100}Sr in the A = 100 beam delivered was more than an order of magnitude higher than the amount of ^{100}Rb, a dipole RF cleaning period of 10 ms was used reduce the amount of isobaric contamination. The comparatively large uncertainty of about 140 keV for our value can therefore be explained by a combination of the preperation time, a poor total system efficiency and, as a consequence of both, the reduction in observed events. Nevertheless, the measurement of ^{100}Rb sets a new record for the shortest-lived isotope to be measured in a Penning trap using HCI.

D. ^{98}Sr

For the Penning-trap mass measurement of ^{98}Sr, [$T_{1/2} = 653(4)$ ms] we find a value of $-62522.4(6.5)$keV for the mass excess. This is within 2σ of the value found by a previous TITAN campaign [12] (87% of the AME 2012 [33, 39] value) and within 1.5σ of the value published by JYFLTRAP [35] (13% of the AME 2012 value). We reanalyzed the value published by TITAN by perfoming a second, independent data analysis, indicating that the deviation is statistical in nature.

E. ^{99}Sr

For the mass excess of ^{99}Sr [$T_{1/2}$ = 269(1) ms] we find a value of $-66416.6(6.7)$keV, which is in agreement with a measurement performed by JYFLTRAP (giving a weight of 24% to the AME 2012 value) in 2006 [35], but agrees only within 2.5σ with a recent TITAN measurement [12] (76% of the AME 2012 [33, 39] value).

We have reanalyzed the data taken during the first TITAN $A \approx 100$ Rb/Sr campaign, arriving at the same mass excess but at a considerably larger uncertainty with ME $(^{99}\mathrm{Sr}) = -62505(19)$ keV. This brings the three existing Penning trap mesaurements into agreement.

F. ^{100}Sr

For ^{100}Sr [$T_{1/2}$ = 202(4) ms] we found a mass excess value of $-59816(12)$ keV, in agreement with the only Penning-trap mass measurement value published to date [35] from JYFLTRAP.

G. ^{101}Sr

We have carried out the first direct mass measurement (see Fig. 2) of ^{101}Sr [$T_{1/2} = 118(3)$ ms] and report a mass excess value of $-55327.6(9.8)$keV. This value marks a 3σ deviation from the one adopted in AME 2012 [33, 39], which is based on the result of a β-endpoint measurement [42] for $^{101}\mathrm{Sr}\,(\beta^-)\,^{101}\mathrm{Y}$. This discrepancy between β-endpoint measurements and PTMS has been documented for neutron-rich isotopes [43].

IV. ASTROPHYSICAL IMPACT

To illustrate the impact of the new data on the r-process in the $A \approx 100$ region of the nuclear chart, we used eq. 1 to calculate fractional abundances in the waiting-point approximation with temperatures 10^8 K $\leq T \leq 10^{10}$ K, neutron densities 10^{18} cm^{-3} $\leq n_n \leq 10^{25}$ cm^{-3} and S_n using data from this work and for comparison S_n from AME 2012 [33, 39]. Values for the partition functions G_i were taken from, or interpolated using a spline function fitted to the data given in, Rauscher et al. [44]. The biggest differences were found for astrophysical conditions with $n_n = 10^{20}$ cm^{-3}, $T = 1.4 \cdot 10^9$K, with waiting points in the $A \approx 100$ region, as illustrated in Fig. 4.

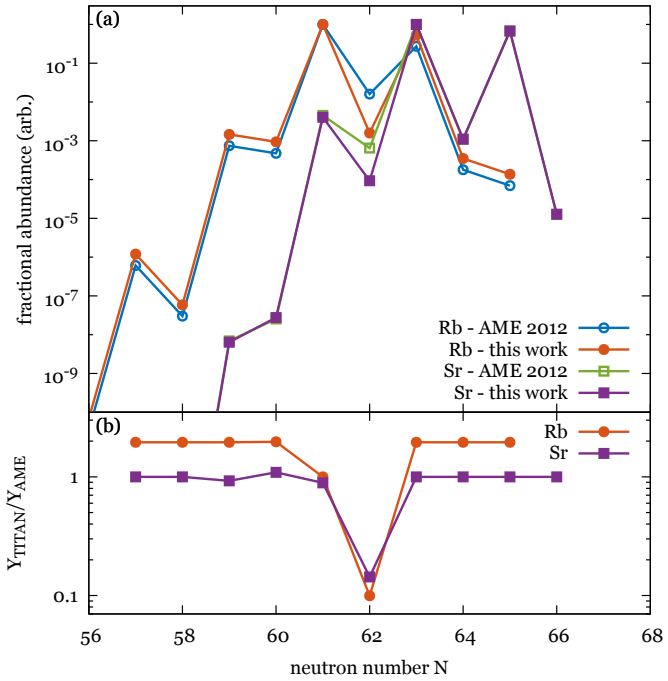

Figure 4. (color online) (a) Fractional r-process abundances, each relative to the most abundant isotope, using the waiting-point approximation for Rb, Sr isotopic-chains with temperature $T = 1.4 \cdot 10^9$ K and neutron density $n_n = 10^{20}$cm^{-3} for S_n from the AME 2012 [33, 39] (squares) and S_n from this work (circles). (b) The ratio $Y_{TITAN}/Y_{AME2012}$ corresponding to the fractional abundances shown in (a).

While the fractional abundances for Rb and Sr with $N = 62$ does change by up to an order of magnitude, the new data do not change the abundance pattern, i.e. location of the waiting points, significantly.

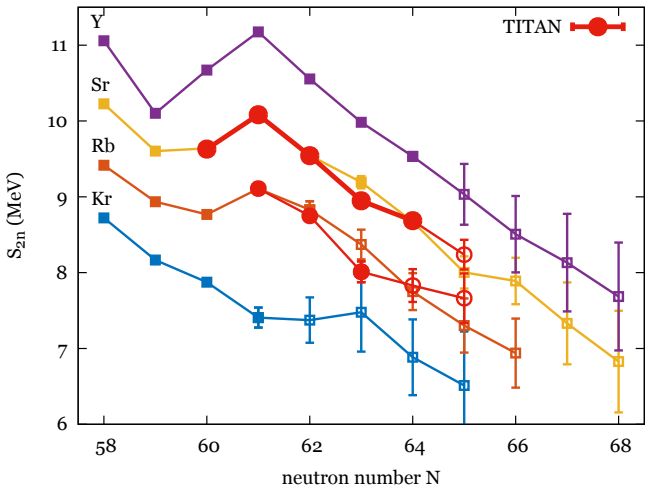

Figure 5. (color online) Two-neutron separation energies for $Z = 36 - 39$ (Kr to Y) versus neutron number. For comparison, S_{2n} based on new TITAN masses are plotted in red circles. S_{2n} graphed with open circles or squares are based on estimated mass values [33, 39].

V. SUMMARY AND FUTURE IMPROVEMENTS

We have measured the masses of ^{98,99}Rb and $^{98-101}$Sr to a precision that makes mass uncertainties negligible for r-process models. The new data do not change the fractional r-process abundance pattern in the $A = 100$ region significantly. We have also presented first mass-spectrometric evidence for a very low-lying isomer in ^{98}Rb. The mass of ^{101}Sr was determined directly for the first time, and the mass determination of ^{99,100}Rb mark a new record for the shortest-lived isotope measured in a Penning trap with HCI. For illustration, the isotopic two-neutron separation energies (S_{2n}) are plotted in Fig. 5 with data from this work and from the Atomic Mass Evaluation 2012 [33, 39].

Mass measurements of isotopes even further from stability were prohibited by a combination of current system efficiency and significant isobaric contamination. Both challenges will be met with the addition of two new traps to the current setup in the near future. A cooler Penning trap (CPET, [45]) will be installed to reduce energy spread and therefore increase capture efficiency as well as signal strength in MPET. To suppress isobaric contamination, a multi-reflection time of flight spectrometer (MR-TOF, [46]) will be installed downstream of the RFQ cooler and buncher with a mass resolving power of up to $m/\Delta m = 50000$. Together these measures should enable TITAN to determine masses of all the neutron-rich Sr and Rb isotopes important for the r-process to a precision, that makes mass-uncertainties neglible for r-process models.

ACKNOWLEDGMENTS

The authors express their gratitude to the TRIUMF technical staff, the ISAC beam delivery group, and M. Good for their contributions in realizing this experiment. This work has been supported by the Natural Sciences and Engineering Research Council of Canada (NSERC) and the National Research Council of Canada. The authors acknowledge financial support for T.D.M. from the NSERC CGS-M program, A.T.G. from the NSERC CGS-D, A.L. from the Deutsche Forschungsgemeinschaft (DFG) under grant FR 601/3-1, and V.V.S. from the Studienstiftung des Deutschen Volkes.

[1] *Connecting Quarks with the Cosmos: Eleven Science Questions for the New Century* (The National Academies

Press, Washington, DC, 2003).
[2] M. Arnould, S. Goriely, and K. Takahashi, Physics Reports **450**, 97 (2007).
[3] F.-K. Thielemann, A. Arcones, R. Käppeli, M. Liebendörfer, T. Rauscher, C. Winteler, C. Fröhlich, I. Dillmann, T. Fischer, G. Martinez-Pinedo, K. Langanke, K. Farouqi, K.-L. Kratz, I. Panov, and I. Korneev, Progress in Particle and Nuclear Physics **66**, 346 (2011), particle and Nuclear Astrophysics International Workshop on Nuclear Physics, 32nd Course.
[4] J. J. Cowan, F.-K. Thielemann, and J. W. Truran, Physics Reports **208**, 267 (1991).
[5] H. Schatz, International Journal of Mass Spectrometry **349-350**, 181 (2013), 100 years of Mass Spectrometry.
[6] E. M. Burbidge, G. R. Burbidge, W. A. Fowler, and F. Hoyle, Rev. Mod. Phys. **29**, 547 (1957).
[7] S. Brett, I. Bentley, N. Paul, R. Surman, and A. Aprahamian, The European Physical Journal A **48**, 184 (2012), 10.1140/epja/i2012-12184-4.
[8] P. Moller, J. Nix, W. Myers, and W. Swiatecki, Atomic Data and Nuclear Data Tables **59**, 185 (1995).
[9] J. Duflo and A. Zuker, Phys.Rev. **C52**, 23 (1995), arXiv:nucl-th/9404019 [nucl-th].
[10] J. Pearson, R. Nayak, and S. Goriely, Physics Letters B **387**, 455 (1996).
[11] R. Rodriguez-Guzman, P. Sarriguren, and L. M. Robledo, Phys. Rev. C **82**, 061302 (2010).
[12] V. V. Simon, T. Brunner, U. Chowdhury, B. Eberhardt, S. Ettenauer, A. T. Gallant, E. Mané, M. C. Simon, P. Delheij, M. R. Pearson, G. Audi, G. Gwinner, D. Lunney, H. Schatz, and J. Dilling, Phys. Rev. C **85**, 064308 (2012).
[13] K. Blaum, J. Dilling, and W. Nörtershauser, Phys.Scripta **T152**, 014017 (2013), arXiv:1210.4045 [physics.atom-ph].
[14] A. A. Kwiatkowski, C. Andreoiu, J. C. Bale, T. Brunner, A. Chaudhuri, U. Chowdhury, P. Delheij, S. Ettenauer, D. Frekers, A. T. Gallant, A. Grossheim, G. Gwinner, F. Jang, A. Lennarz, T. Ma, E. Mané, M. R. Pearson, B. E. Schultz, M. C. Simon, V. V. Simon, and J. Dilling, Hyperfine Interactions **225**, 143 (2014).
[15] J. Dilling, R. Baartman, P. Bricault, M. Brodeur, L. Blomeley, F. Buchinger, J. Crawford, J. C. López-Urrutia, P. Delheij, M. Froese, G. Gwinner, Z. Ke, J. Lee, R. Moore, V. Ryjkov, G. Sikler, M. Smith, J. Ullrich, and J. Vaz, International Journal of Mass Spectrometry **251**, 198 (2006).
[16] J. Dilling, R. Krücken, and G. Ball, in *ISAC and ARIEL: The TRIUMF Radioactive Beam Facilities and the Scientific Program*, edited by J. Dilling, R. Krücken, and L. Merminga (Springer Netherlands, 2014) pp. 1–8.
[17] P. Kunz, P. Bricault, M. Dombsky, N. Erdmann, V. Hanemaayer, J. Wong, and K. Lützenkirchen, Journal of Nuclear Materials **440**, 110 (2013).
[18] P. Bricault, F. Ames, M. Dombsky, P. Kunz, and J. Lassen, in *ISAC and ARIEL: The TRIUMF Radioactive Beam Facilities and the Scientific Program* (Springer Netherlands, 2014) pp. 25–49.
[19] T. Brunner, M. Smith, M. Brodeur, S. Ettenauer, A. Gallant, V. Simon, A. Chaudhuri, A. Lapierre, E. Mané, R. Ringle, M. Simon, J. Vaz, P. Delheij, M. Good, M. Pearson, and J. Dilling, Nuclear Instruments and Methods in Physics Research Section A: Accelerators, Spectrometers, Detectors and Associated Equipment **676**, 32 (2012).
[20] M. Smith, L. Blomeley, P. Delheij, and J. Dilling, Hyperfine Interactions **173**, 171 (2006).
[21] A. Lapierre, M. Brodeur, T. Brunner, S. Ettenauer, A. Gallant, V. Simon, M. Good, M. Froese, J. C. López-Urrutia, P. Delheij, S. Epp, R. Ringle, S. Schwarz, J. Ullrich, and J. Dilling, Nuclear Instruments and Methods in Physics Research Section A: Accelerators, Spectrometers, Detectors and Associated Equipment **624**, 54 (2010).
[22] T. Brunner, A. Mueller, K. O'Sullivan, M. Simon, M. Kossick, S. Ettenauer, A. Gallant, E. Mané, D. Bishop, M. Good, G. Gratta, and J. Dilling, International Journal of Mass Spectrometry **309**, 97 (2012).
[23] M. König, G. Bollen, H.-J. Kluge, T. Otto, and J. Szerypo, International Journal of Mass Spectrometry and Ion Processes **142**, 95 (1995).
[24] M. Brodeur, V. Ryjkov, T. Brunner, S. Ettenauer, A. Gallant, V. Simon, M. Smith, A. Lapierre, R. Ringle, P. Delheij, M. Good, D. Lunney, and J. Dilling, International Journal of Mass Spectrometry **310**, 20 (2012).
[25] S. Ettenauer, M. C. Simon, A. T. Gallant, T. Brunner, U. Chowdhury, V. V. Simon, M. Brodeur, A. Chaudhuri, E. Mané, C. Andreoiu, G. Audi, J. R. C. López-Urrutia, P. Delheij, G. Gwinner, A. Lapierre, D. Lunney, M. R. Pearson, R. Ringle, J. Ullrich, and J. Dilling, Phys. Rev. Lett. **107**, 272501 (2011).
[26] S. Malbrunot-Ettenauer, T. Brunner, U. Chowdhury, A. T. Gallant, V. V. Simon, M. Brodeur, A. Chaudhuri, E. Mané, M. C. Simon, C. Andreoiu, G. Audi, J. R. Crespo López-Urrutia, P. Delheij, G. Gwinner, A. Lapierre, D. Lunney, M. R. Pearson, R. Ringle, J. Ullrich, and J. Dilling, Phys. Rev. C **91**, 045504 (2015).
[27] D. Frekers, M. Simon, C. Andreoiu, J. C. Bale, M. Brodeur, T. Brunner, A. Chaudhuri, U. Chowdhury, J. C. López-Urrutia, P. Delheij, H. Ejiri, S. Ettenauer, A. T. Gallant, V. Gavrin, A. Grossheim, M. N. Harakeh, F. Jang, A. A. Kwiatkowski, J. Lassen, A. Lennarz, M. Luichtl, T. Ma, T. D. Macdonald, E. Mané, D. Robertson, B. Schultz, V. V. Simon, A. Teigelhöfer, and J. Dilling, Physics Letters B **722**, 233 (2013).
[28] S. Ettenauer, M. Simon, T. Macdonald, and J. Dilling, International Journal of Mass Spectrometry **349 - 350**, 74 (2013), 100 years of Mass Spectrometry.
[29] A. Kellerbauer, K. Blaum, G. Bollen, F. Herfurth, H.-J. Kluge, M. Kuckein, E. Sauvan, C. Scheidenberger, and L. Schweikhard, The European Physical Journal D - Atomic, Molecular, Optical and Plasma Physics **22**, 53 (2003).
[30] K. Blaum, D. Beck, G. Bollen, P. Delahaye, C. Gu'enaut, F. Herfurth, A. Kellerbauer, H.-J. Kluge, D. Lunney, S. Schwarz, L. Schweikhard, and C. Yazidjian, EPL (Europhysics Letters) **67**, 586 (2004).
[31] G. Rodrigues, P. Indelicato, J. Santos, P. Patté, and F. Parente, Atomic Data and Nuclear Data Tables **86**, 117 (2004).
[32] M. Brodeur, T. Brunner, C. Champagne, S. Ettenauer, M. Smith, A. Lapierre, R. Ringle, V. L. Ryjkov, G. Audi, P. Delheij, D. Lunney, and J. Dilling, Phys. Rev. C **80**, 044318 (2009).
[33] M. Wang, G. Audi, A. Wapstra, F. Kondev, M. MacCormick, X. Xu, and B. Pfeiffer, Chinese Physics C **36**, 1603 (2012).

[34] V. Manea, D. Atanasov, D. Beck, K. Blaum, C. Borgmann, R. B. Cakirli, T. Eronen, S. George, F. Herfurth, A. Herlert, M. Kowalska, S. Kreim, Y. A. Litvinov, D. Lunney, D. Neidherr, M. Rosenbusch, L. Schweikhard, F. Wienholtz, R. N. Wolf, and K. Zuber, Phys. Rev. C **88**, 054322 (2013).

[35] U. Hager, T. Eronen, J. Hakala, A. Jokinen, V. S. Kolhinen, S. Kopecky, I. Moore, A. Nieminen, M. Oinonen, S. Rinta-Antila, J. Szerypo, and J. Äystö, Phys. Rev. Lett. **96**, 042504 (2006).

[36] G. Lhersonneau, B. Pfeiffer, R. Capote, J. M. Quesada, H. Gabelmann, and K.-L. Kratz, Phys. Rev. C **65**, 024318 (2002).

[37] A. T. Gallant, M. Brodeur, T. Brunner, U. Chowdhury, S. Ettenauer, V. V. Simon, E. Mané, M. C. Simon, C. Andreoiu, P. Delheij, G. Gwinner, M. R. Pearson, R. Ringle, and J. Dilling, Phys. Rev. C **85**, 044311 (2012).

[38] T. Procter, J. Behr, J. Billowes, F. Buchinger, B. Cheal, J. Crawford, J. Dilling, A. Garnsworthy, A. Leary, C. Levy, E. Mané, M. Pearson, O. Shelbaya, M. Stolz, W. Al Tamimi, and A. Voss, The European Physical Journal A **51**, 23 (2015), 10.1140/epja/i2015-15023-2.

[39] G. Audi, M. Wang, A. Wapstra, F. Kondev, M. MacCormick, X. Xu, and B. Pfeiffer, Chinese Physics C **36**, 1287 (2012).

[40] G. Audi, A. Coc, M. Epherre-Rey-Campagnolle, G. L. Scornet, C. Thibault, and F. Touchard, Nuclear Physics A **449**, 491 (1986).

[41] R. Iafigliola, H. Dautet, S. W. Xu, J. K. P. Lee, R. Chrien, R. Gill, and M. Shmid, Proceedings of the 7th International, Conference Atomic Masses and Fundamental Constants AMCO–7 , 141 (1984).

[42] K. Balog, M. Graefenstedt, M. Groß, P. Jürgens, U. Keyser, F. Münnich, T. Otto, F. Schreiber, T. Winkelmann, and J. Wulff, Zeitschrift für Physik A Hadrons and Nuclei **342**, 125 (1992).

[43] J. Van Schelt, D. Lascar, G. Savard, J. A. Clark, S. Caldwell, A. Chaudhuri, J. Fallis, J. P. Greene, A. F. Levand, G. Li, K. S. Sharma, M. G. Sternberg, T. Sun, and B. J. Zabransky, Phys. Rev. C **85**, 045805 (2012).

[44] T. Rauscher and F.-K. Thielemann, Atomic Data and Nuclear Data Tables **75**, 1 (2000).

[45] Z. Ke, W. Shi, G. Gwinner, K. Sharma, S. Toews, J. Dilling, and V. Ryjkov, Hyperfine Interactions **173**, 103 (2006).

[46] C. Jesch, T. Dickel, W. R. Plaß, D. Short, S. Ayet San Andres, J. Dilling, H. Geissel, F. Greiner, J. Lang, K. G. Leach, W. Lippert, C. Scheidenberger, and M. I. Yavor, Hyperfine Interactions , 1 (2015).